Asian Journal of Chemistry; Vol. 38, No. 7 (2026), 1930-1946
ASIAN JOURNAL OF CHEMISTRY
https://doi.org/10.14233/ajchem.2026.36117

Micronutrient-Fortified Guar Gum-Borax Hydrogels for Controlled Release and Improved Growth of Green Gram (*Vigna radiata*)

JINALI B. SHAH[1,*], K. SANTHOSH KUMAR[1] and PUJAN B. VAISHNAV[2]

[1]Department of Chemical Sciences, School of Science, GSFC University, Vadodara-391750, India
[2]Research & Development Centre, Gujarat State Fertilizers & Chemicals Limited, Vadodara-391750, India

*Corresponding author: E-mail: jinali3095@gmail.com

Received: 1 April 2026 *Accepted*: 20 June 2026 *Published online*: 3 July 2026 AJC-22418

Micronutrient deficiencies and water scarcity are major constraints to crop productivity, especially in conditions of excessive cultivation and low fertilizer use efficiency. To overcome this, the designing of smart materials such as hydrogels by simple and scalable synthesis method is essential. In this study, we propose the development of fortified guar gum-borax (GGB) hydrogels as polysaccharide-derived matrices for controlled micronutrient delivery. Different loading strategies were investigated to incorporate essential micronutrients, including Zn, Fe, Mn, Cu and B, into the hydrogel matrix. Among the approaches evaluated, the post-gelation loading method proved to be the most effective for achieving efficient nutrient encapsulation and retention. Comprehensive physico-chemical characterization confirmed the successful incorporation of the micronutrients within the hydrogel network. Furthermore, soil incubation and aqueous release studies demonstrated a sustained and controlled release behaviour confirmed prolonged micronutrient availability and enhanced nutrient delivery potential. Pot trials on green gram (*Vigna radiata*) revealed that fortified hydrogel treatments showed faster germination and better or comparable vegetative growth when compared with treatments of conventional micronutrient fertilisation. Post-harvest soil analysis indicated that fortified-GGB hydrogels-maintained soil pH and electrical conductivity within a comparable range while supporting post-harvest micronutrient availability.

Keywords: Guar gum-borax hydrogels, Micronutrient delivery, Controlled release, Green gram, Sustainable agriculture.

INTRODUCTION

Micronutrient deficiencies in agricultural soils represent a major global challenge, significantly limiting crop productivity and threatening food security worldwide. Due to an intensive cropping system to fulfil the food requirements of an increasing population, nutrient contents of essential micro-elements like zinc (Zn), iron (Fe), boron (B), manganese (Mn) and copper (Cu) are reduced in soils, which leads to decrease in plant growth and yield across variety of crops [1,2]. Due to these, staple crops are unable to supply enough nutrient content, which affects the nutritional quality of the food [3]. Micronutrients are essential elements for physiological processes of plants like enzyme activation, photosynthesis, nitrogen metabolism and redox balance [4]. Even in trace amounts, micronutrients have significant impacts on plant growth, root development, reproduction processes and response to stress [5].

Conventional salts or chelated forms of micronutrients are usually used as fertilizers to balance nutrient levels in soils. They usually have faster dissolution rate, which can cause fixation or leaching in soil, leading to poor nutrient use efficiency [6]. These fertilizer salts can easily precipitate out with soil constituents or get washed away during irrigation, making them less available at the root zone right after application [7]. In response to these challenges, hydrogels have been increasingly explored as controlled nutrient-release carriers owing to their three-dimensional cross-linked architecture and versatile functional properties. In agriculture, hydrogels serve as efficient water-retention reservoirs, capable of swelling upon water absorption and subsequently releasing the stored water in a controlled manner over prolonged periods through diffusion [8]. Hydrogels have been reported to improve soil water retention, thereby reducing irrigation demands [6]. In addition, their ability to act as nutrient carriers facilitates controlled and prolonged nutrient release, mitigating losses through

leaching and improving nutrient-use efficiency compared to traditional fertilizers [7]. Furthermore, polysaccharide-based hydrogels derived from starch, cellulose, chitosan and alginate are promising materials for sustainable agriculture due to their biodegradability, non-toxicity and biocompatibility. These biopolymer-based hydrogels can be tailored to achieve desired swelling and nutrient-release properties, providing an eco-friendly alternative to synthetic hydrogels for efficient water and nutrient management [8-10].

For sustainable agricultural applications, polysaccharide based hydrogels have attracted considerable attention due to their biodegradability, biocompatibility and environmentally benign nature. Among these, guar gum (GG), a galactomannan polysaccharide obtained from *Cyamopsis tetragonoloba*, is a promising biopolymer for hydrogel synthesis owing to its abundance of hydroxyl groups that readily interact with cross-linking agents such as borax [11,12]. Structurally, guar gum consists of a β-(1→4)-linked mannose backbone with galactose side chains, imparting high hydrophilicity and enabling the formation of extensive hydrogen-bonded and borate cross-linked networks through borate–diol complexation [13]. The resulting hydrogels exhibit high porosity, excellent water absorption capacity and pH-responsive swelling behaviour, making them suitable carriers for controlled nutrient delivery and moisture management in soil systems [14-16].

Several studies have demonstrated the potential of guar gum-based hydrogels in agricultural and environmental applications. For example, boron-loaded guar gum hydrogels have been reported as effective systems for the sustained release of boron [17]. Nevertheless, the development of biodegradable hydrogel matrices capable of simultaneously delivering multiple essential micronutrients remains largely unexplored. Current controlled-release fertilizers (CRFs) are commonly produced by coating nutrient sources with inorganic materials or synthetic and natural polymers to regulate nutrient availability [18]. More recently, nutrient-loaded hydrogels have emerged as promising alternatives for the controlled release of both macro- and micronutrients. However, most existing studies focus on single-nutrient formulations, underscoring the need for multifunctional hydrogel systems capable of delivering multiple nutrients while maintaining structural stability and controlled-release performance [19-21].

The incorporation of nutrients during hydrogel synthesis can influence polymer network formation, nutrient distribution and release behavior. Furthermore, achieving desired nutrient ratios and predictable release profiles remains challenging. For instance, multilayer hydrogel fertilizer systems containing Cu, Mn and Zn immobilized on biopolymer matrices often face limitations related to homogeneous nutrient loading and sustained release over extended periods [22,23]. Consequently, there is a pressing need for simple, scalable and eco-friendly strategies for incorporating multiple micronutrients into biodegradable hydrogel networks without compromising their structural and functional properties.

In the present study, guar gum–borax (GGB) hydrogels fortified with individual micronutrients (Zn, Fe, Mn, Cu and B) as well as multi-micronutrient formulations were developed and evaluated. The fortified hydrogels were characterized for elemental composition, structural integrity, morphology and thermal stability. Nutrient release behaviour in soil and aqueous media was investigated using diffusion-based kinetic models. Furthermore, pot experiments using green gram (*Vigna radiata*) were conducted to compare the performance of fortified hydrogels with conventional micronutrient fertilizers by assessing seed germination, plant growth, and post-harvest soil nutrient status. The findings highlight the potential of guar gum-derived hydrogels as biodegradable soil amendments for sustained micronutrient delivery and improved soil moisture and nutrient management.

EXPERIMENTAL

All chemicals and reagents were of analytical grade and used as received. Certified green gram (*Vigna radiata*) seeds were procured from a local agro-seed supplier. Guar gum and sodium tetraborate (borax) were used for preparation of the GGB hydrogel. Micronutrient sources used for hydrogel fortification were EDTA (ethylenediamine tetraacetic acid) salts of Zn, Fe, Cu, Mn, disodium octaborate tetrahydrate (DOT) and micronutrient-mix (MNM) for the multi-micronutrient formulation. Urea and diammonium phosphate (DAP) were used for soil and pot studies. Deionised water was used throughout the study.

Synthesis of fortified-GGB-hydrogels: Initial guar gum-borax (GGB) hydrogel was synthesised by adopting modified procedure [24]. For micronutrient incorporation, solutions of EDTA-chelated micronutrients Fe-EDTA, Cu-EDTA, Mn-EDTA, Zn-EDTA and MNM (containing 6% Zn, 4% Fe, 0.5% Cu, 1% Mn, 0.5% B) were prepared separately at pH 8 (adjusted with dilute NaOH). Based on soil application requirements (1-10 kg ha^{-1}), the quantities of each micronutrient source were calculated for a hydrogel application rate of 5 kg ha^{-1} as shown in Table-1.

Three approaches were evaluated for micronutrient incorporation into GGB hydrogel matrix, for example, (i) **Co-precipitation:** pre-mixing borax and micronutrient solutions and then addition to guar gum solution; (ii) **Pre-dispersion:** sequential addition of micronutrient and then borax solutions

TABLE-1
QUANTITIES OF MICRONUTRIENT SOURCES FOR FORTIFICATION OF GUAR-GUM-BORAX (GGB) HYDROGELS

Fortified hydrogel	Micronutrient source	Quantity (mg)	Elemental content (mg)	Rationale (kg ha^{-1} soil rate)
Fe-GGB hydrogel	Fe-EDTA	100	~13 Fe	5-10 Fe
Cu-GGB hydrogel	Cu-EDTA	25	~3.5 Cu	1-2 Cu
Mn-GGB hydrogel	Mn-EDTA	50	~6.5 Mn	3-5 Mn
Zn-GGB hydrogel	Zn-EDTA	150	~18 Zn	~5 Zn
MNM-GGB hydrogel	Micronutrient-mix	300	Fe ~12, Zn ~18, Mn ~3, Cu ~1.5, B ~1.5	Composite needs

to guar gum solution (iii) **Post-gelation:** addition of micronutrient solutions into pre-formed GGB hydrogel mixture. After selecting the optimal approach, five independent batches of freshly prepared GGB hydrogels were prepared, each designated for loading of one type of micronutrient solution. The micronutrient solutions were then slowly added to the guar gum-borax mixture under moderate stirring for 30 min to achieve equilibration and kept stable for about 12 h to ensure uniform diffusion and binding of micronutrient with GGB hydrogel structure. The resulting micronutrient-loaded hydrogels (Fe-GGB, Cu-GGB, Mn-GGB, Zn-GGB and MNM-GGB) were filtered by nylon sieve, washed with distilled water, dried at 40-45 ºC and stored in airtight containers for subsequent characterisation and soil application studies.

Nutrient incorporation efficiency: To confirm nutrient incorporation, ICP-OES analysis of both GGB and fortified-GGB-hydrogels was conducted using an Avio 200 instrument (Perkin-Elmer, USA). Sample solutions were prepared by wet acid digestion procedure and analysed for micronutrient concentration expressed in mg kg^{-1} (ppm). The percentage incorporation of each micronutrient was determined according to the procedure published [25,26].

Characterisation of micronutrient-fortified GGB hydrogels: FT-IR spectra of the micronutrient-fortified GGB hydrogels were recorded using an IRSpirit FT-IR spectrophotometer (Shimadzu, Japan) equipped with a diamond ATR accessory over the range of 4000-400 cm^{-1}. All measurements were performed on dry powdered samples at room temperature, with a fresh background scan acquired before each analysis. Thermal stability and degradation behaviour were evaluated by thermogravimetric analysis (TGA) and derivative thermogravimetry (DTG) using a TGA-4000 thermogravimetric analyser (Perkin-Elmer, USA). Samples were heated from 25 to 620 ºC at a rate of 5 ºC min^{-1} under a nitrogen atmosphere. X-ray diffraction (XRD) analysis was conducted using a D8 Advance diffractometer (Bruker, Germany) to investigate the structural and phase characteristics of the hydrogels. Finely powdered samples were mounted on zero-background holders and scanned over an appropriate 2θ range. Surface morphology and elemental composition were examined by scanning electron microscopy coupled with energy-dispersive X-ray spectroscopy (SEM-EDS) using a Nova NanoSEM 450 microscope (FEI Ltd., USA) equipped with an XFlash 7 EDS detector (Bruker, Germany). Prior to analysis, samples were sputter-coated with gold and examined at an accelerating voltage of 20 kV.

Swelling behaviour: Swelling behaviour of GGB hydrogel was evaluated in deionised water, 0.9% NaCl and buffer solutions of pH 4.0, 7.0 and 9.2. A known quantity of dried hydrogel was incubated in the selected swelling medium and collected at predefined time points. Surface-adhered liquid was gently removed using absorbent paper and the swollen hydrogel was weighed immediately to assess water uptake and swelling capacity. The swelling index was calculated using the following equation:

$$\text{Swelling index (g/g)} = \frac{W_t - W_o}{W_o}$$

where W_o is the initial dry weight of hydrogel; and W_t is the swollen weight at time t.

Nutrient release kinetics in water: Micronutrient release from GGB and fortified-GGB-hydrogels was examined in deionised water and compared to equivalent conventional sources. Accurately weighed samples of 0.5 g fortified hydrogels and matching elemental amounts from conventional fertilizers, disodium octaborate tetrahydrate (DOT) and EDTA salts (Fe-, Cu-, Mn-, Zn-EDTA) were added in separate 250 mL Erlenmeyer flasks containing 150 mL deionised water in each. A blank was kept for background elemental levels. The flasks were kept at 25 ± 1 ºC in an incubator with 25 rpm shaking for 120 h. At definite intervals (1, 2, 4, 6, 12, 24, 48, 72, 96, 120 h), 5 mL aliquots were withdrawn as samples. To maintain sink conditions, after each sample withdrawal, 5 mL of fresh deionised water was added to each flask. Samples were filtered through 0.45 μm membrane filters prior to elemental analysis for B, Zn, Fe, Mn and Cu concentrations (ICP-OES 5110, Agilent Technologies, USA). The cumulative release was calculated as a percentage of total loaded nutrient content relative to conventional sources. Results are reported in means ± standard deviations from triplicate experiments.

Nutrient release kinetics in soil: A composite soil sample was prepared by mixing equal proportions of air-dried clay, sandy and loamy soils, then sieved through a 2 mm mesh to remove debris and ensure uniformity. For each treatment, 1 kg of this processed soil was placed in perforated plastic pots fitted with drainage holes. The soil was initially amended with the recommended dose of fertilizers (RDF; 100 mg urea and 222 mg diammonium phosphate kg^{-1} soil) to establish the control treatment (T1: RDF alone). For hydrogel-based treatments, GGB, Zn-GGB, Fe-GGB, Cu-GGB, Mn-GGB and MNM-GGB hydrogels were enclosed in nylon mesh bags and buried in the RDF-amended soil to facilitate nutrient diffusion while preventing direct contact with the soil matrix. In the conventional fertilizer treatments, micronutrient sources equivalent to the elemental content of the respective hydrogels were thoroughly mixed with the soil, including DOT (15 mg; ~3 mg B kg^{-1} soil), Zn-EDTA (28 mg; ~4 mg Zn kg^{-1}), Fe-EDTA (39 mg; ~5 mg Fe kg^{-1}), Mn-EDTA (48 mg; ~5 mg Mn kg^{-1}), Cu-EDTA (24 mg; ~2 mg Cu kg^{-1}) and a micronutrient mixture (50 mg providing ~5 mg each of Zn, Fe, and Mn, and ~1 mg each of Cu and B kg^{-1} soil). The pots were incubated at 25 ± 1 ºC, with soil moisture maintained at field capacity by weekly addition of distilled water. Soil subsamples (20 g) were collected at 0, 1, 3, 7, 14, 21, 30, 45 and 60 days, air-dried, sieved (< 0.5 mm) and extracted with AB-DTPA solution by shaking for 30 min at 120 rpm and 25 ºC. The extracts were filtered through Whatman No. 42 filter paper, and the concentrations of B, Zn, Fe, Mn, and Cu were quantified using ICP-OES. All results are presented as mean ± standard deviation of three independent replicates.

Pot trials on green gram (*Vigna radiata*): The pot trial experiment was conducted using plastic pots fitted with drainage perforations at the bottom. Each pot was filled with approximately 2.5 kg of air-dried soil mixture comprising clayey, sandy and loamy soils in suitable proportions. Prior to sowing, the composite soil sample was analysed for its initial physico-chemical properties and elemental content to check its suitability for conducting pot trials. Soil pH was determined in a 1:2.5 soil-to-water suspension and electrical

conductivity (EC) was measured using the same extract. Soil organic carbon (OC) content was estimated by the Walkley-Black wet oxidation method employing a colorimetric method and elemental content was analysed using ICP-OES. Absolute control and treatment T_1 with RDF (urea + diammonium phosphate) kept under the same conditions without conventional fertiliser and hydrogel treatments served as a comparison. A total of fourteen treatment groups were established in triplicate for the pot trials. Treatments T_3, T_5, T_7, T_9, T_{11} and T_{13} received RDF with fortified hydrogels. Treatments T_2, T_4, T_6, T_8, T_{10} and T_{12} were fertilised with RDF and conventional micronutrient sources. The treatment details are as summarised in Table-2. The experimental design included an absolute control, RDF control, blank GGB hydrogel control, conventional micronutrient treatments and corresponding fortified GGB hydrogel treatments. The blank GGB treatment was included to distinguish the effect of the guar gum-borax hydrogel matrix from micronutrient fortification. The conventional micronutrient treatments were used as nutrient-matched comparators for evaluating hydrogel-based delivery.

Germination count: Each treatment consisted of three replications with 20 seeds per pot. *V. radiata* seeds were sown in moist soil at a depth of 2.5 cm. A 100 mL of water was added to each pot regularly in order to maintain adequate soil moisture which is critical for seed germination and initial seedling growth. An absolute control and RDF (T_1) were incorporated for comparative analysis. Equal sunlight exposure was provided to each treatment pot throughout the study. The germinated seeds were counted as the first and final count on the 7th and 10th day, respectively. The following eqn. was used to calculate the germination percentage.

$$\text{Germination (\%)} = \frac{\text{Number of seeds germinated}}{\text{Total number of seeds sown}} \times 100$$

Morphological parameters: After 60 days of sowing, plant growth parameters of *V. radiata* were assessed to understand impact of conventional fertilizers *vs.* fortified hydrogel treatments compared with absolute control and RDF. Three representative plant samplings were taken from each pot of each treatment group, uprooted from soil and washed to get rid of excess dirt and particles. Various morphological and growth attributes, including root length, shoot length, total plant height, vigor index, leaf dimensions (length and width), leaf area, fresh biomass and dry biomass, were evaluated to quantify root development, vegetative growth and plant productivity. Fresh biomass was measured right after the harvest while dry biomass was measured after drying plant samplings until constant weight is achieved. Vigor index was calculated using % gemination and total of root and shoot length.

Vigor index = % Germination × Seedling length (cm)

Post-harvest soil study: Post-harvest soil samples from each treatment were collected after plant removal and air-dried. Post-harvest soil samples were analyzed for pH, electrical conductivity (EC), organic carbon (OC) and available nutrient concentrations to assess the influence of hydrogel-based treatments on soil chemical characteristics and nutrient status after crop cultivation.

Statistical analysis: All experiments with replicate-level data were analysed as mean ± standard deviation (n = 3). One-way analysis of variance (ANOVA) was used to evaluate treatment effects on germination, morphological and post-harvest soil properties. For matched comparisons between conventional micronutrient sources and corresponding fortified GGB hydrogel treatments, Welch's t-test was applied. Differences were considered statistically significant at $p < 0.05$. Nutrient release profiles were evaluated by fitting the experimental data to appropriate kinetic models. As the release experiments comprised single time-series measurements, the results were interpreted descriptively rather than subjected to replicate-based statistical analyses.

RESULTS AND DISCUSSION

The formation of the guar gum-borax (GGB) hydrogels was developed by borate-diol crosslinking between the hydroxyl rich guar gum backbone and borate species generated from borax in an aqueous medium. The galactomannan polysaccharide, guar gum, contains many vicinal hydroxyl groups that are capable of interacting with tetrahydroxyborate species in slightly alkaline conditions [27].

TABLE-2
TREATMENT DETAILS OF GREEN GRAM (*Vigna radiata*) POT TRIAL (2.5 KG SOIL PER POT, ha^{-1})

Code	Treatment	Application per pot
AC	Absolute control (A.C.)	Soil only
T_1	RDF	0.28 g urea + 0.55 g DAP
T_2	RDF + B (DOT*)	RDF + 0.07 g DOT (1 kg B $ha^{-1\#}$)
T_3	RDF + GGB	RDF + 0.22 g GGB (20 kg ha^{-1})
T_4	RDF + Zn-EDTA	RDF + 0.28 g Zn-EDTA (5 kg Zn)
T_5	RDF + Zn-GGB	RDF + 0.25-0.30 g Zn-GGB (5 kg Zn)
T_6	RDF + Micronutrient-mix	RDF + 0.28 g Micronutrient-Mix
T_7	RDF + MNM-GGB	RDF + 0.25-0.30 g MNM-GGB
T_8	RDF + Fe-EDTA	RDF + 0.55 g Fe-EDTA (10 kg Fe)
T_9	RDF + Fe-GGB	RDF + 0.25-0.35 g Fe-GGB (10 kg Fe)
T_{10}	RDF + Cu-EDTA	RDF + 0.14 g Cu-EDTA (2.5 kg Cu)
T_{11}	RDF + Cu-GGB	RDF + 0.20-0.25 g Cu-GGB (2.5 kg Cu)
T_{12}	RDF + Mn-EDTA	RDF + 0.25-0.30 g Mn-EDTA (5 kg Mn)
T_{13}	RDF + Mn-GGB	RDF + 0.25-0.30 g Mn-GGB (5 kg Mn)

*DOT : Disodium octaborate tetrahydrate; $^{\#}ha^{-1}$: Per hectare

As shown in **Scheme-I**, borax dissolves in water to form borate ions, which then interact with adjacent hydroxyl groups of guar gum to form borate ester linkages. These dynamic B-O-C bridges connect neighbouring polymer chains, forming a three-dimensional hydrogel network, as demonstrated by the immediate gelation observed upon dropwise addition of borax. This crosslinking process transforms the hydrated polymer solution into a viscoelastic and water-retentive matrix suitable for micronutrient encapsulation. Interaction of *cis*-diol groups present in the guar gum chains with borate ions causes the gelation process. This produces temporary supramolecular crosslinks instead of permanent covalent bonds. The resulting hydrogel possesses an oxygen-rich and highly hydrated microenvironment, which is favourable for subsequent micronutrient loading. The bonds of the borate ester compound are reversible and this property is significant as it imparts structural flexibility, swelling characteristics and diffusion pathways essential for the absorption and controlled retention of metal-containing species. This dynamic network, therefore, acts not only as a hydrogel scaffold but also as a chemically interactive host system.

Micronutrients were retained within the GGB hydrogel matrix mainly through physical entrapment within the crosslinked polymeric network and possible interactions with oxygen-containing functional groups of guar gum and borate-associated groups. They penetrate the structure of hydrogel and get entrapped within its cross-linked polymeric matrix. The hydroxyl groups of guar gum and borate-mediated linkages provide potential interaction sites for metal-containing species. The proposed interaction mechanism is therefore supported by indirect evidence from ICP-OES, FT-IR, TGA, XRD, SEM-EDS characterisation and the observed controlled nutrient release profiles. **Scheme-II** illustrates that the oxygen donor atoms within the hydroxyl groups of guar gum, along with the borate-associated oxygens, present potential interaction sites for metal species. This characteristic allows the hydrogel to act as a polymer that can incorporate metals within its matrix. Among the three loading methods studied, the post-gelation loading technique showed the best chemical stability. This approach maintained the borate-mediated network, thereby promoting more uniform diffusion and retention of micronutrient species without interfering with the initial gelation chemistry. The pH of the micronutrient solutions was kept at 8.0. At this pH, borate species retain adequate reactivity with the hydroxyl groups of guar gum and the EDTA-chelated micronutrients remain soluble, thereby minimising the occurrence of hydrolysis or precipitation. Subsequent drying of the loaded hydrogels at 40-45 ºC likely induced partial contraction of the polymeric network, further entrapping the micronutrient species within the matrix.

Fortified-GGB-hydrogel was synthesised as shown in Fig. 1. Where approaches A and B produced gels with non-uniform structure due to the precipitation, phase separation or aggregation due to interference of metal cations with borate-diol crosslinking. Approach C produced consistent and stable hydrogels and was selected as the optimal technique for integrating micronutrients into the hydrogel matrix.

Nutrient incorporation efficiency: The micronutrient composition of GGB and fortified-GGB hydrogels was determined by ICP-OES and the results are shown in Tables 3 and 4. The unfortified GGB hydrogel contained boron originating from borax used as the crosslinking agent, while Fe,

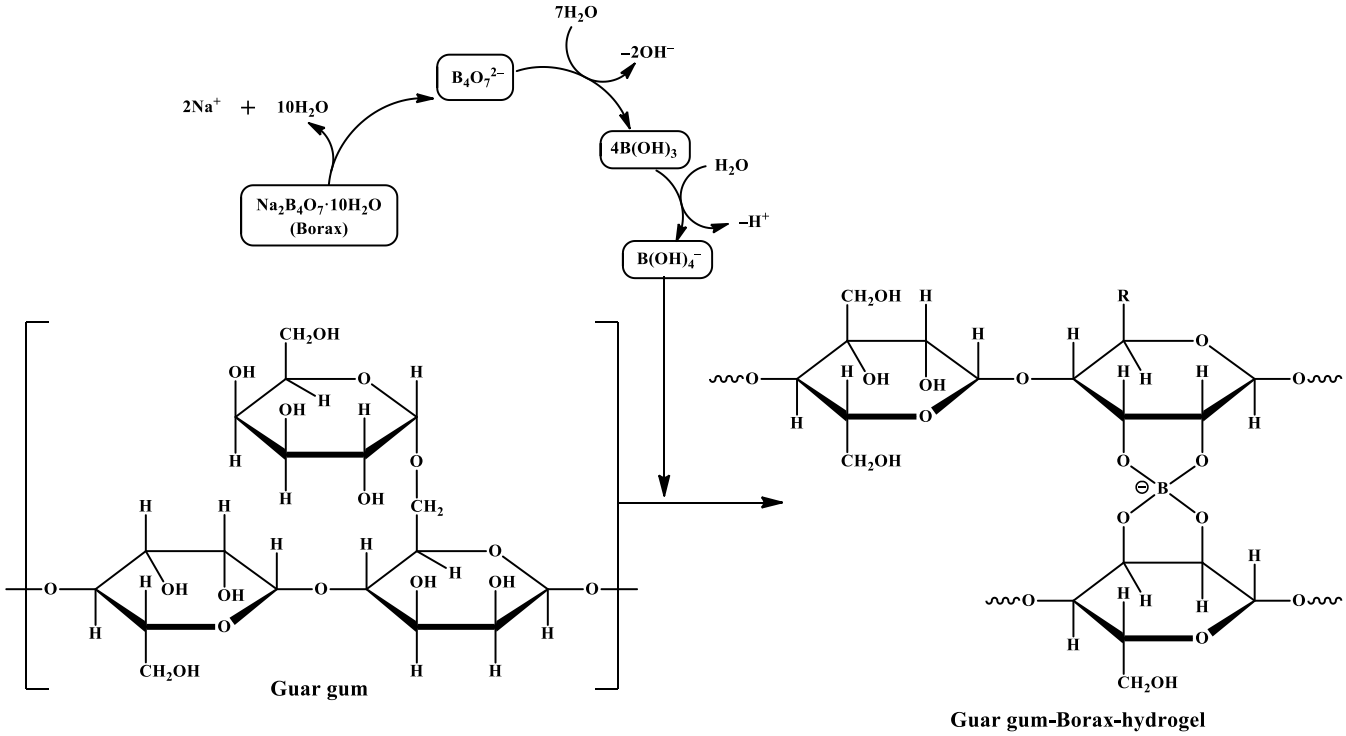

Scheme-I: Schematic representation of borax dissociation in aqueous medium and subsequent borate-mediated crosslinking of guar gum to form guar gum-borax (GGB) hydrogel

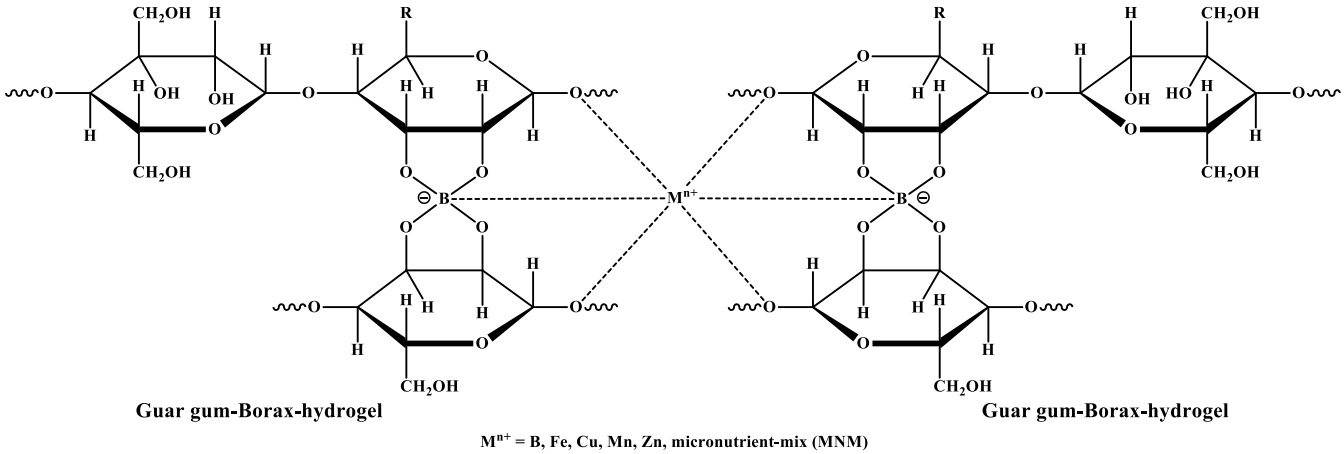

Scheme-II: Proposed interaction of micronutrient ions [M^{n+} = B, Fe, Cu, Mn, Zn, Micronutrient-Mix (MNM)] with the guar gum-borax (GGB) hydrogel network through coordination with oxygen-containing functional groups

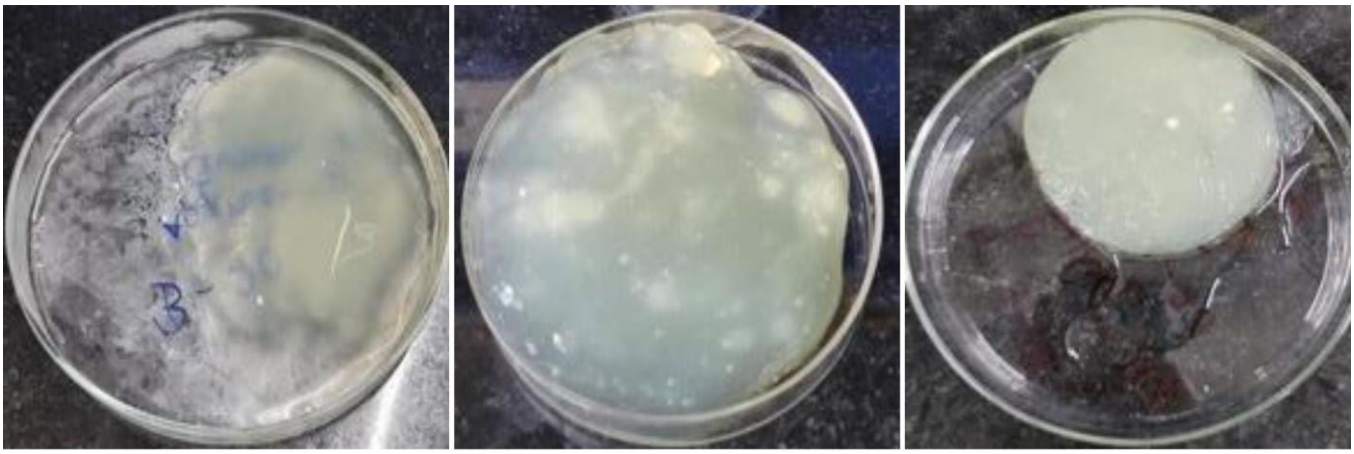

Fig. 1. Visual representation of fortified hydrogel prepared with different methods

TABLE-3
ICP-OES METAL CONCENTRATION IN HYDROGELS (mg kg^{-1})

Hydrogel	B	Fe	Cu	Mn	Zn
GGB	22862.0	ND	ND	ND	ND
Fe-GGB	17811.0	4460.3	ND	ND	ND
Cu-GGB	20932.0	ND	1212.1	ND	ND
Mn-GGB	18893.0	ND	ND	2284.3	ND
Zn-GGB	13664.0	ND	ND	ND	6127.9
MNM-GGB	9984.9	4896.8	344.58	511.82	3836.5

TABLE-4
HYDROGEL YIELD, MICRONUTRIENT ADDITION, ICP-OES RESULTS AND INCORPORATION EFFICIENCY

Hydrogel	Hydrogel yield (g)	Source	Elemental metal added (mg)	ICP (mg kg^{-1})	ICP Metal in 100 mg sample	Incorporation (%)
GGB hydrogel	0.75	Borax	2.25 (B)	22862	2.286	101.6
Fe-GGB hydrogel	0.82	Fe-EDTA	13 (Fe)	4460.3	0.446	99.0
Zn-GGB hydrogel	0.85	Zn-EDTA	18 (Zn)	6127.9	0.613	101.0
Cu-GGB hydrogel	0.80	Cu-EDTA	3.5 (Cu)	1212.1	0.121	98.6
Mn-GGB hydrogel	0.83	Mn-EDTA	6.5 (Mn)	2284.3	0.228	99.1
MNM-GGB hydrogel	0.88	Micronutrient-mix	1.5 (B)	9984.9	0.998	100.2
			12 (Fe)	4896.8	0.490	99.5
			18 (Zn)	3836.5	0.384	100.0
			1.5 (Cu)	344.58	0.0345	101.5
			3 (Mn)	511.82	0.0512	100.1

Cu, Mn and Zn were either absent or present only at trace levels. In contrast, the respective fortified hydrogels (Fe-GGB, Zn-GGB, Cu-GGB, Mn-GGB and MNM-GGB) exhibited substantial concentrations of their target micronutrients, confirming successful incorporation into the hydrogel matrix. The measured micronutrient concentrations closely matched the theoretical loading levels signifying efficient nutrient retention during hydrogel preparation. Incorporation efficiencies ranged from 95% to 102% across all formulations. The single-micronutrient hydrogels showed incorporation efficiencies of 99.0% for Fe, 101.0% for Zn, 98.6% for Cu and 99.1% for Mn, while boron retention remained approximately 100%. Similarly, the multi-micronutrient hydrogel (MNM-GGB) exhibited incorporation efficiencies of 100.2% for B, 99.5% for Fe, 100.0% for Zn, 101.5% for Cu and 100.1% for Mn. These results demonstrate that the post-gelation fortification approach enabled highly efficient and reproducible loading of micronutrients into the GGB hydrogel network.

Characterisation of GGB and fortified-GGB-hydrogels

FT-IR analysis: The FT-IR overlay spectra of GGB and micronutrient-fortified GGB hydrogels are shown in Fig. 2. The broad absorption band observed at ~3419 cm^{-1}, corresponding to O–H stretching vibrations of the crosslinked galactomannan network, exhibited a gradual decrease in intensity following micronutrient incorporation. This change suggests the involvement of hydroxyl groups in interactions between the hydrogel matrix and loaded micronutrients. Similarly, the band near 1650 cm^{-1} showed reduced intensity, indicating possible interactions between metal ions and functional groups within the hydrogel network. The characteristic bands at ~1420 cm^{-1} and ~1070 cm^{-1}, assigned to symmetric $–COO^-$ stretching and C–O–C/C–O vibrations of the guar gum backbone, respectively, remained evident but displayed slight variations in intensity and position after fortification, reflecting changes in the local chemical environment. In addition, a weak absorption band appeared near 550 cm^{-1} in the fortified hydrogels, which may be attributed to metal–oxygen (M–O) vibrations. The observed changes in FT-IR spectra are consistent with successful micronutrient loading within the GGB hydrogel matrix, supporting the elemental composition data and highlighting the potential of these hydrogels for sustained nutrient delivery [28].

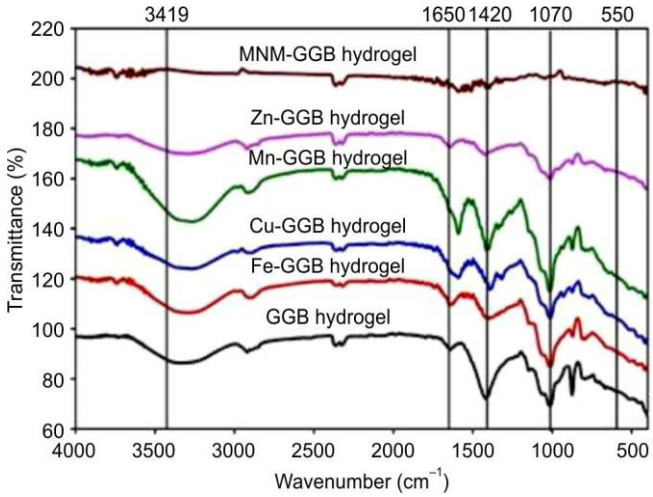

Fig. 2. FT-IR spectra of GGB and fortified-GGB hydrogels

Thermal studies: Thermogravimetric analysis (TGA) and derivative thermogravimetry (DTG) were employed to evaluate the thermal stability and decomposition behaviour of GGB and micronutrient-fortified GGB hydrogels. All samples exhibited three distinct stages of weight loss: (i) removal of moisture and volatile components (30-250 ºC), (ii) degradation of the polysaccharide backbone (250-400 ºC) and (iii) formation of residual char above 400 ºC, characteristic of crosslinked polysaccharide-based hydrogels (Fig. 3). Weight loss up to 250 ºC ranged from 14 wt.% for the GGB hydrogel to 25.5 wt.% for the fortified hydrogels, demonstrating an increased moisture retention following micronutrient incorporation (Table-5).

The major degradation step occurred at T_{max} values between 281.1 and 291.9 ºC. The GGB hydrogel exhibited the highest T_{max} (291.9 ºC), whereas the fortified hydrogels showed slightly lower T_{max} values (281.1-288.0 ºC), signifying minor

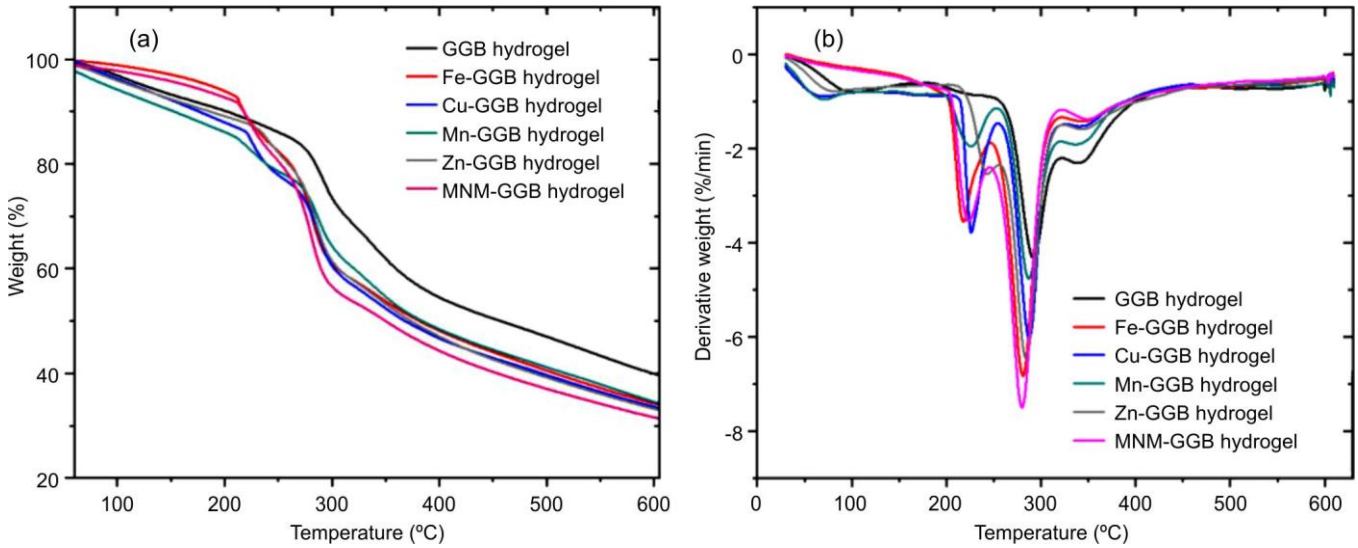

Fig. 3. (a) TGA and (b) DTG profiles of GGB and fortified-GGB-hydrogels

TABLE-5
THERMAL DECOMPOSITION PARAMETERS OF GGB AND FORTIFIED-GGB-HYDROGELS

Sample	Moisture loss (wt.%)*	T_{max} (ºC)#	DTG peak height (%/min)	Residue (wt.%) (600 ºC)
GGB-hydrogel	14.0	291.9	3.48	39.9
Fe-GGB-hydrogel	17.6	281.1	5.19	34.3
Cu-GGB-hydrogel	24.5	287.6	4.56	31.3
Mn-GGB-hydrogel	21.4	287.2	3.67	34.6
Zn-GGB-hydrogel	25.5	284.0	5.26	32.0
MNM-GGB-hydrogel	18.8	288.0	4.0	32.3

*Calculated as (100 - wt.% at 250 ºC); #Temperature of maximum DTG peak

changes in the thermal stability after micronutrient loading. Despite these shifts, all fortified hydrogels retained comparable decomposition profiles confirmed the preservation of the hydrogel network structure. Char residue at 600 ºC decreased from 39.9 wt.% for the GGB hydrogel to 31.3-34.6 wt.% for the fortified formulations. The moderate differences in degradation behaviour and residual mass suggest successful micronutrient incorporation without substantial alteration of the hydrogel matrix. The observed thermal behaviour indicates that the fortified hydrogels retain their structural stability following micronutrient incorporation, highlighting their suitability for agricultural nutrient delivery applications [29].

Crystallinity analysis (XRD): Changes in the structural characteristics of GGB and micronutrient-fortified GGB hydrogels were investigated using XRD analysis (Fig. 4). The GGB hydrogel exhibited a broad diffraction peak centered at 2θ ≈ 20.4º indicate the predominantly amorphous nature of the borax-crosslinked guar gum network. Following the micronutrient fortification, all hydrogels retained this characteristic amorphous profile, the principal diffraction peak within a narrow range (2θ ≈ 20.6-20.9º), confirmed that micronutrient incorporation did not alter the underlying hydrogel structure. In addition to the broad amorphous peak, weak reflections appeared at higher diffraction angles in the fortified hydrogels, attributable to localized crystalline domains associated with the incorporated metal–EDTA complexes. Fe-GGB and Zn-GGB exhibited minor secondary reflections around 29-31º, while Cu-GGB displayed relatively more pronounced peaks at 29.5º, 31.1º, 43.3 º and 50.5º. Mn-GGB showed only a weak high-angle reflection, which is due to the limited crystalline nature, whereas the MNM-GGB hydrogel exhibited a combined features arising from the presence of multiple micronutrients. The persistence of the broad amorphous peak together with the appearance of low-intensity crystalline reflections confirms that micronutrient fortification introduced localized ordered domains without disrupting the amorphous guar gum-borax network, confirmed the successful incorporation of micronutrients while preserving the structural characteristics of the hydrogel matrix required for sustained nutrient delivery [30].

Morphological and elemental studies: FE-SEM and EDS: SEM images (Fig. 5a-f) display distinct morphological evolution of GGB hydrogel to its fortified variants. GGB hydrogel (a) exhibits a highly porous, irregular and fibrous network which is typical of crosslinked galactomannan polysaccharides, with interconnected macropores, which is a suitable characteristic for soil amendment for water retention in soil [31]. While fortification of micronutrients induces modifications in porosity and surface uniformity. Fe-GGB (b) and Cu-GGB (c) are having smoother surfaces and reduced fibrous structure suggesting that metal ions might have enhanced borax crosslinking density. Mn-GGB (d) and Zn-GGB (e) show a more compact surface with finer porosity, while the multi-nutrient MNM-GGB (f) combines all these characteristics and has a uniform, less heterogeneous structure. These changes in morphology confirm that micronutrient incorporation stabilizes the hydrogel framework, making it a more stable crosslink structure.

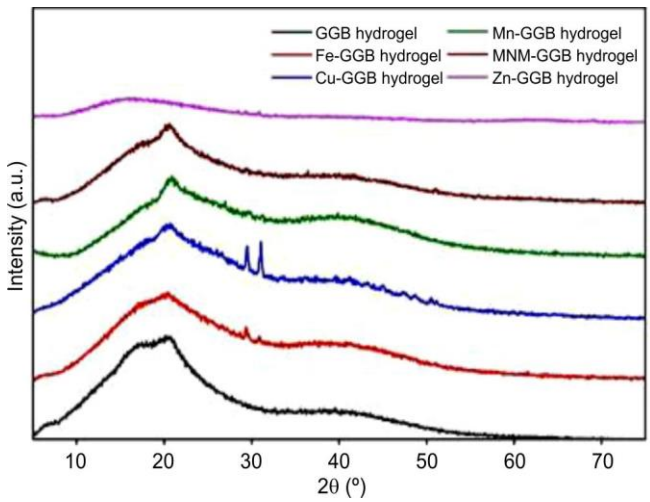

Fig. 4. XRD patterns of GGB and fortified-GGB-hydrogels

The EDX spectra (Fig. 6a-f) confirmed the presence of Fe, Cu, Mn, and Zn in the respective fortified hydrogels, whereas these elements were absent or present only at trace levels in the unfortified GGB hydrogel. These findings support the successful incorporation of micronutrients into the hydrogel matrix and are consistent with the morphological changes observed in the SEM images. The combined SEM-EDX analysis indicates that micronutrient fortification modifies both the composition and microstructure of the GGB hydrogel while maintaining its integrity, making it a promising material for controlled nutrient delivery in agricultural applications.

Swelling behaviour of GGB hydrogel: The GGB hydrogel showed medium-dependent swelling behaviour (Table-6). The maximum swelling index was observed in deionised water (57.60 g/g at 2 h), followed by pH 4 buffer (38.11 g/g at 12 h), pH 9.2 buffer (34.48 g/g at 2 h), pH 7 buffer (26.44 g/g at 12 h) and 0.9% NaCl solution (23.56 g/g at 2 h). The lower swelling in NaCl solution suggests that ionic strength reduced water uptake, probably due to the charge screening and reduced osmotic driving force. These results support the water-

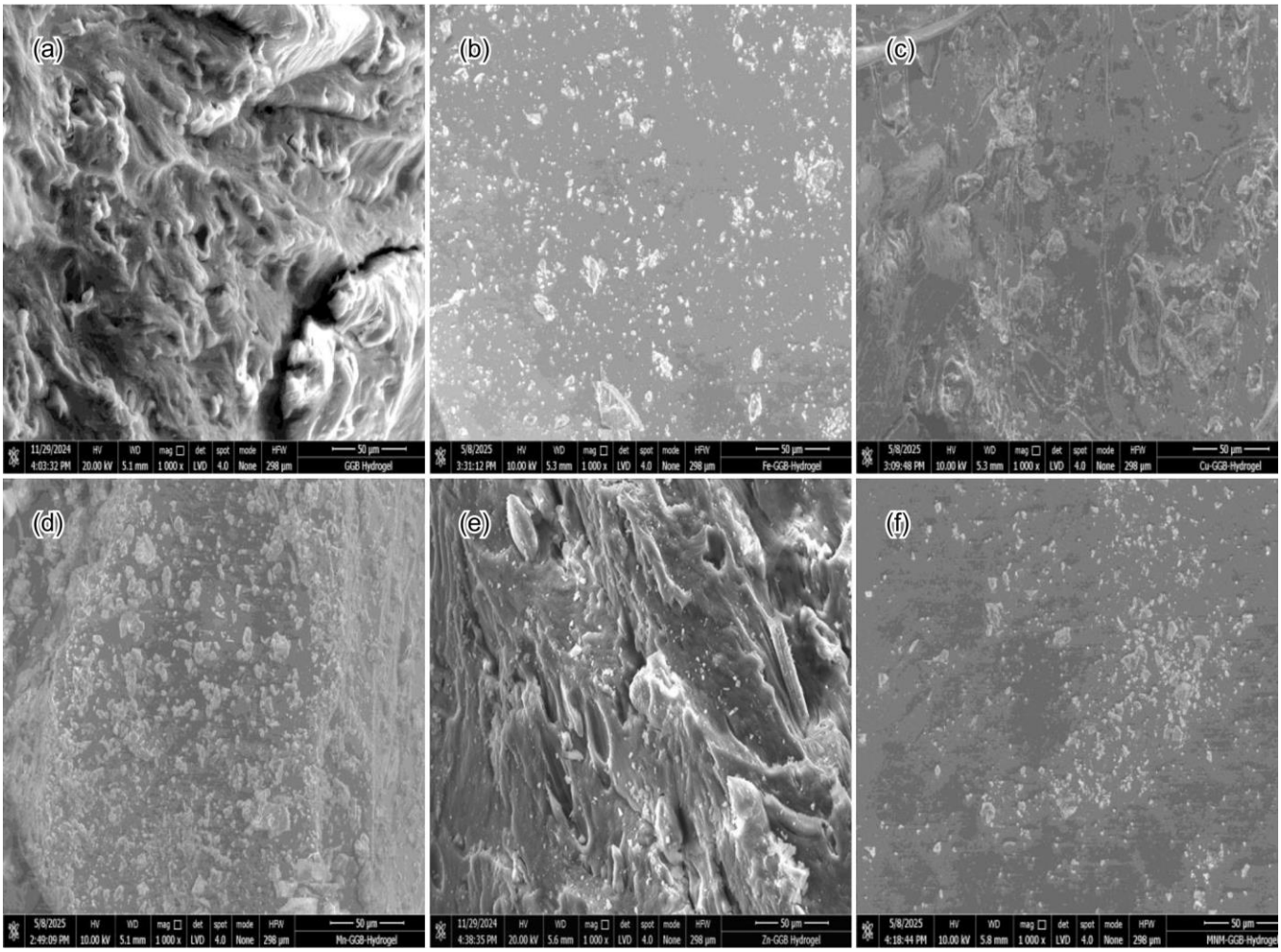

Fig. 5. SEM micrographs of (a) GGB hydrogel, (b) Fe-GGB-hydrogel, (c) Cu-GGB-hydrogel, (d) Mn-GGB-hydrogel, (e) Zn-GGB-hydrogel, (f) MNM-GGB-hydrogel [Scale bars: 50 μm (all at 1000×)]

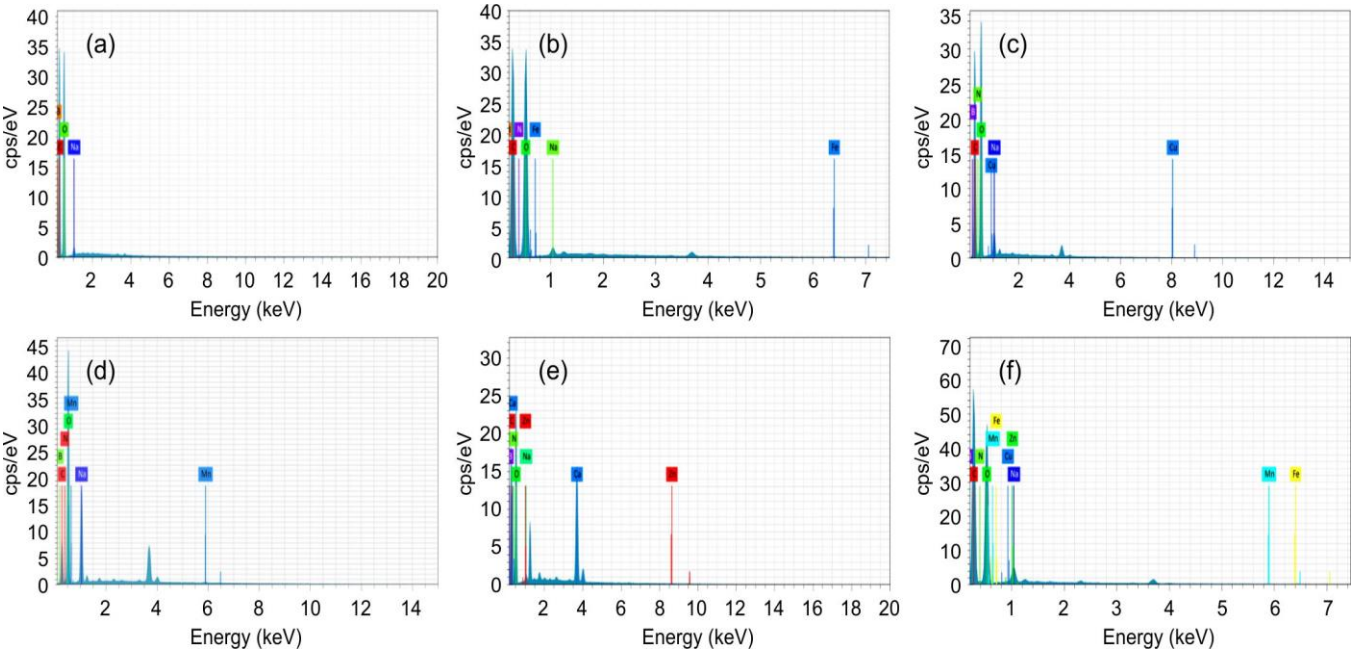

Fig. 6. EDS spectra of (a) GGB-hydrogel, (b) Fe-GGB-hydrogel, (c) Cu-GGB-hydrogel, (d) Mn-GGB-hydrogel (e) Zn-GGB-hydrogel and (f) MNM-GGB-hydrogel

TABLE-6
MAXIMUM SWELLING INDEX OF
GGB HYDROGEL IN DIFFERENT MEDIA

Medium	Maximum swelling index (g/g)	Time at maximum (h)	12 h swelling index (g/g)
DM Water	57.60	2	44.48
0.9% NaCl	23.56	2	19.64
pH 4	38.11	12	38.11
pH 7	26.44	12	26.44
pH 9.2	34.48	2	33.02

absorbing nature of the GGB hydrogel and provide experimental support for its role as a diffusion-based micronutrient carrier.

Nutrient release in water: The aqueous release behaviour of micronutrients from GGB hydrogels was evaluated in comparison with their corresponding conventional fertilizer sources under identical conditions [17]. The increasing nutrient release profiles in water revealed distinct differences between conventional micronutrient sources and hydrogel-based formulations (Fig. 7a-j). Conventional micronutrient salts exhibited rapid dissolution, with more than 60-75% of the nutrient content released within the first 1-2 h and nearly complete release (>95%) within 12-24 h, reflecting their characteristic burst-release behaviour. In contrast, all fortified GGB hydrogels displayed a controlled and sustained release pattern extending up to 120 h, accompanied by a substantially reduced initial release rate.

The unfortified GGB hydrogel showed gradual boron release, reaching approximately 89-90% increased release after 120 h. Similarly, Fe-GGB, Cu-GGB, Mn-GGB, and Zn-GGB hydrogels released 74-86% of their respective micronutrient contents over the same period. The slower release from fortified hydrogels can be attributed to interactions between the incorporated micronutrients and the guar gum–borax network, which retard nutrient diffusion through the hydrogel matrix. Differences in cumulative release among micronutrients were also observed, reflecting variations in ion mobility and interactions with the polymer network. Mn and Zn exhibited relatively higher cumulative release, whereas Fe and Cu showed comparatively slower release rates.

The multi-micronutrient hydrogel (MNM-GGB) exhibited a similar sustained-release pattern for all incorporated nutrients. Although slight differences were observed among individual micronutrients, the final release behaviour remained controlled throughout the experimental period. After 120 h, increased release followed the order B (~89%) > Mn (~87%) > Zn (~84%) > Cu (~78%) > Fe (~74%). Compared with the corresponding micronutrient mixture, MNM-GGB effectively reduced the initial burst effect and prolonged nutrient availability, highlighting its potential as a multi-nutrient delivery system.

The statistical comparison of nutrient concentrations released at 120 h further confirmed the controlled-release characteristics of the fortified hydrogels. The concentrations released from hydrogel formulations were significantly lower than those from their corresponding conventional micronutrient sources (Welch's t-test, $p < 0.001$). At 120 h, the measured concentrations were 17.77 ± 0.14 mg L^{-1} for boron from GGB hydrogel compared with 22.49 ± 0.07 mg L^{-1} from DOT, 8.86 ± 0.20 mg L^{-1} for Fe-GGB compared with 15.17 ± 0.12 mg L^{-1} for the conventional Fe source, 11.91 ± 0.08 mg L^{-1} for Mn-GGB compared with 17.40 ± 0.35 mg L^{-1} for the conventional Mn source, 8.01 ± 0.13 mg L^{-1} for Cu-GGB compared with 14.11 ± 0.18 mg L^{-1} for the conventional Cu source, and 7.72 ± 0.14 mg L^{-1} for Zn-GGB compared with 16.24 ± 0.18 mg L^{-1} for the conventional Zn source.

To elucidate the release mechanism, the experimental release data were fitted to the Korsmeyer–Peppas kinetic model (Table-7). Excellent linearity was obtained for all formulations, with correlation coefficients (R^2) ranging from approximately 0.96 to 0.98, indicating a good fit of the model to the experimental data. The diffusion exponent (n) values ranged from 0.42 to 0.49 and remained below 0.5 for all formulations, suggesting that nutrient release predominantly followed a Fickian diffusion mechanism. These results indicate that water penetration into the hydrogel matrix is followed by diffusion of the incorporated micronutrients through the hydrated polymer network. Variations in the kinetic constant (k) among different micronutrients further reflect differences in nutrient mobility and interactions within the hydrogel structure. Thus, the observed release behaviour highlights the ability of micronutrient-fortified GGB hydrogels to regulate nutrient delivery and maintain extended nutrient availability in comparison with conventional fertilizer sources.

Nutrient release in soil: The soil incubation study across fortified-GGB-hydrogels compared to conventional fertilizers revealed distinct release patterns of micronutrients (Table-8 and Fig. 8a-f). The absolute control and RDF-only (T_1) treatments maintained native baseline levels: Zn 0.47-

TABLE-7
KORSMEYER-PEPPAS KINETIC PARAMETERS FOR MICRONUTRIENTS RELEASE

Hydrogel	Nutrient	n (diffusion exponent)	k (kinetic constant)	R^2	Type of diffusion
GGB	B	0.41	0.14	0.976	Fickian diffusion
Fe-GGB	Fe	0.48	0.09	0.979	Fickian diffusion
Cu-GGB	Cu	0.51	0.08	0.980	Quasi-Fickian
Mn-GGB	Mn	0.47	0.10	0.971	Fickian diffusion
Zn-GGB	Zn	0.44	0.11	0.973	Fickian diffusion
MNM-GGB	B	0.42	0.137	0.979	Fickian diffusion
	Fe	0.48	0.090	0.968	Fickian diffusion
	Cu	0.49	0.082	0.983	Fickian diffusion
	Mn	0.46	0.106	0.975	Fickian diffusion
	Zn	0.46	0.105	0.977	Fickian diffusion

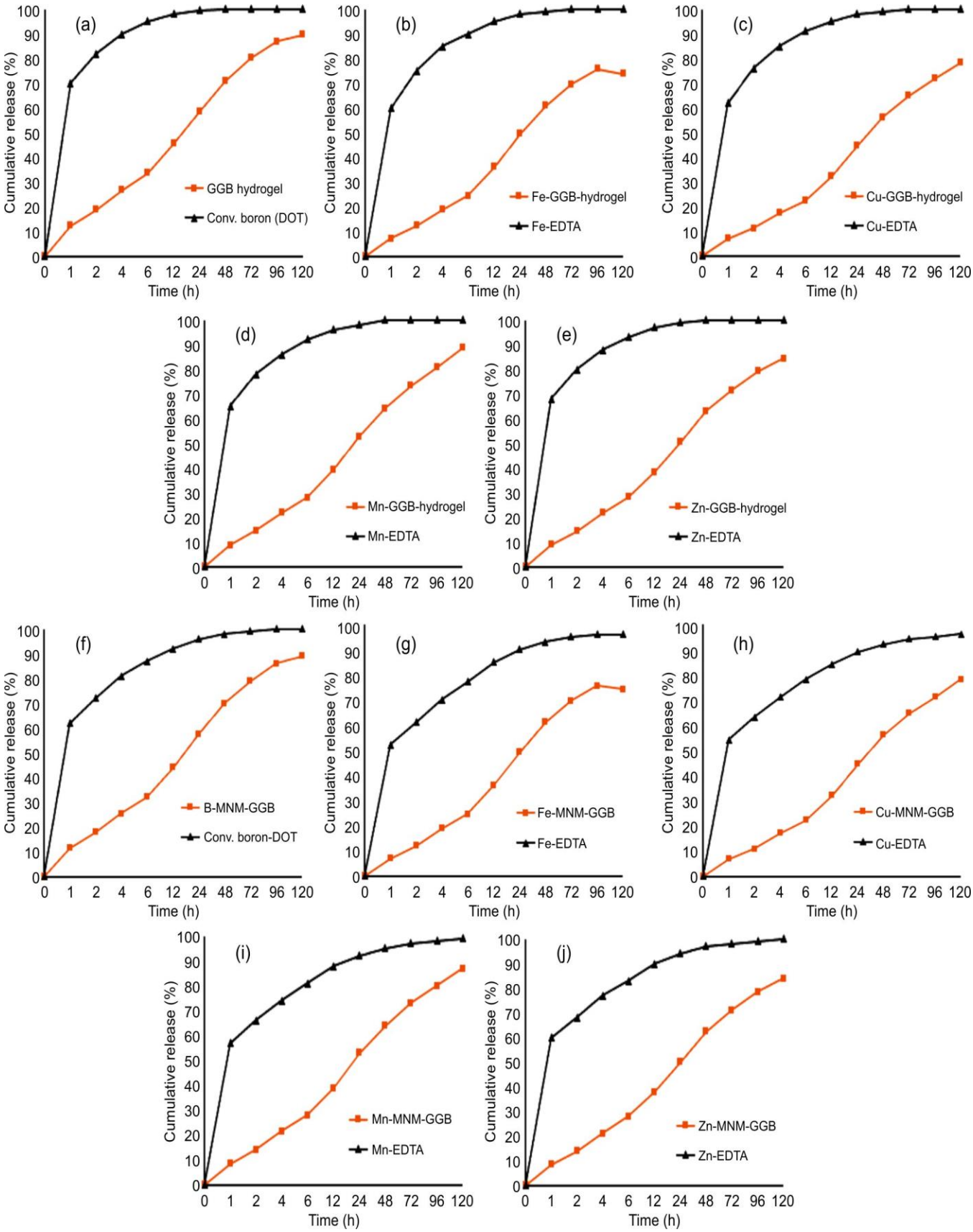

Fig. 7. Cumulative release (%) of (a) B from GGB hydrogel, (b) Fe from Fe-GGB hydrogel, (c) Cu from Cu-GGB hydrogel, (d) Mn from Mn-GGB-hydrogel, (e) Zn from Zn-GGB hydrogel, (f) B from MNM-GGB hydrogel, (g) Fe from MNM-GGB hydrogel, (h) Cu from MNM-GGB hydrogel, (i) Mn from MNM-GGB hydrogel, and (j) Zn from MNM-GGB hydrogel in water

TABLE-8
CUMULATIVE MICRONUTRIENTS RELEASE (%) AT DAY 7 AND DAY 60 FOR CONVENTIONAL *versus* HYDROGEL TREATMENTS

Micronutrient	Day 7 Conv. (mg kg^{-1}/%)	Day 7 hydrogel (mg kg^{-1}/%)	Day 60 conv. (mg kg^{-1}/%)	Day 60 hydrogel (mg kg^{-1}/%)
B (T_2 *vs*. T_3)	0.48/90	0.50/48	0.48/98	0.50/88
Zn (T_4 *vs*. T_5)	5.1/95	4.6/85	5.1/100	4.6/95
Fe (T_8 *vs*. T_9)	5.1/90	4.5/80	5.1/98	4.5/92
Mn (T_{12} *vs*. T_{13})	5.1/92	4.6/82	5.1/99	4.6/94
Cu (T_{10} *vs*. T_{11})	2.1/85	1.8/75	2.1/95	1.8/88
Micronutrient-mix (T_6 *vs*. T_7)	1.1/80	0.9/70	1.1/90	0.9/85

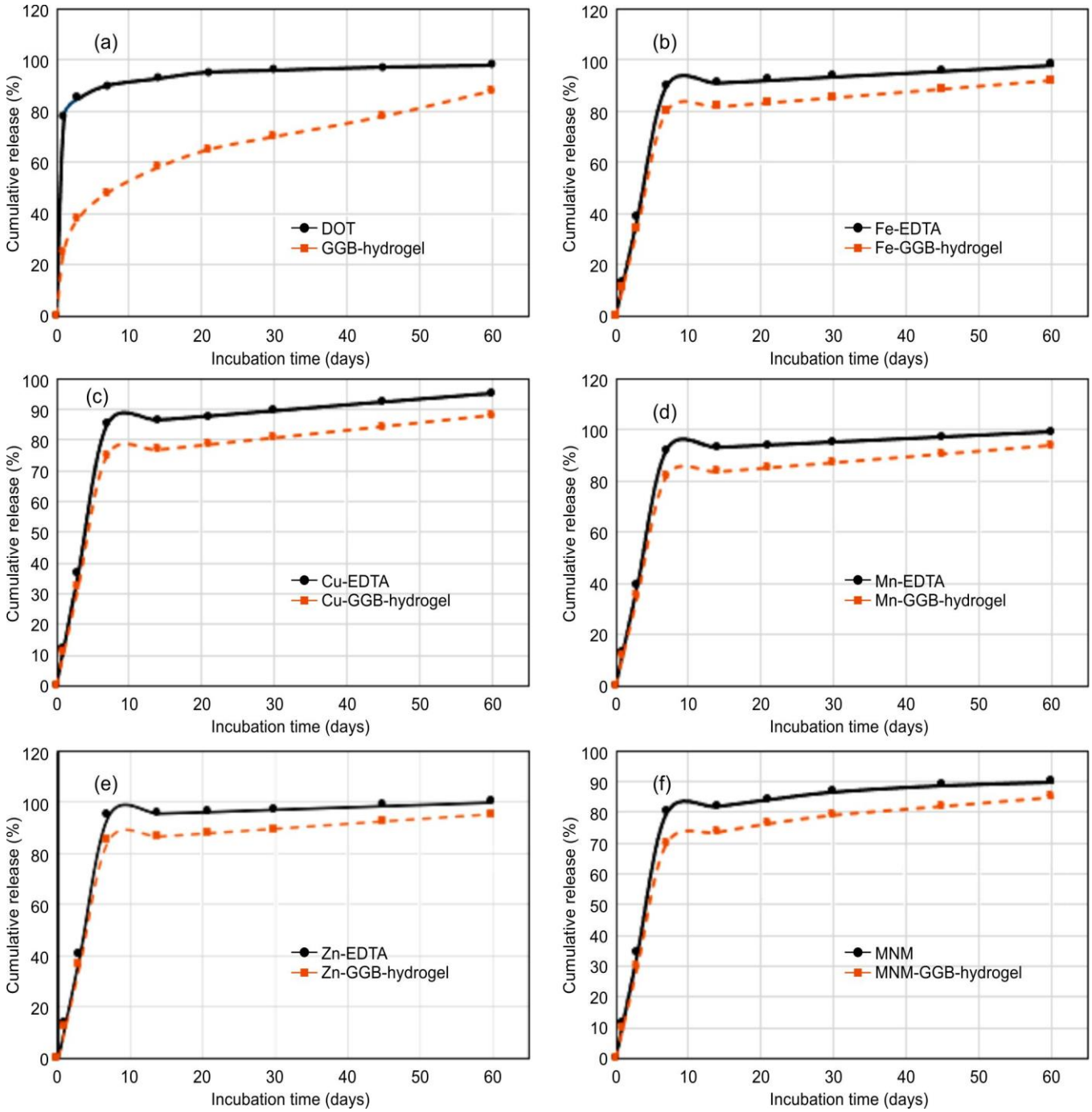

Fig. 8. Cumulative release profiles and kinetics fitted to first order model for (a) GGB hydrogel (b) Fe-GGB hydrogel (c) Cu-GGB hydrogel (d) Mn-GGB-hydrogel (e) Zn-GGB hydrogel (f) MNM-GGB hydrogel over 60 days in soil

0.53, Fe 3.07-3.08, Mn 1.07, Cu 0.28-0.31 and B 0.48-0.51 mg kg^{-1} over a duration of 60 days. Treatments of conventional fertiliser salts (T_4, T_8, T_{10} and T_{12}) showed immediate release of nutrients on day 0, reaching over 85% by day 7. GGB hydrogel treatments (T_5, T_9, T_{11}, T_{13}) initiated at marginally reduced concentrations and displayed a gradual release, reaching 75-95% cumulative release by day 60. Multi-nutrient formulations showed that MNM-GGB (T_7) outperformed micronutrient-mix (T_6), providing a balanced supply of Zn, Fe, Mn, Cu and B without excessive early spikes. Soil quality parameters remained consistent across treatments with pH ranged from 6.8 to 6.9; organic carbon 0.60% to 0.63% and electrical conductivity 0.15 to 0.22 dS m^{-1}.

Traditional micronutrient salts exhibited burst kinetics, which is indicative of rapid dissolution, with typical release rate constants of 0.35 day^{-1} ($r^2 \geq 0.995$) (Table-9). This excessive availability of nutrients in the initial stage after application generates soluble ion pools which are susceptible to leaching during irrigation, precipitation, or fixation by soil phosphates and carbonates, particularly in alkaline soils. On the contrary, GGB hydrogels demonstrated a release rate 1.4-2.2 times slower (mean k = 0.24 day^{-1}; $r^2 > 0.96$), governed by the Fickian diffusion of EDTA-metal complexes through the guar polysaccharide matrix, which supports controlled and sustained nutrient release. This polymer-controlled mechanism regulates ion transport by dynamic borate diol crosslinks and matrix relaxation, forming the linear sigmoidal profiles that aligns nutrient supply with crop demand throughout vegetative stages. The superior first-order kinetic fits for nutrients establish matrix diffusion as the rate-limiting factor. These findings demonstrate that fortified-GGB-hydrogels can be used as excellent slow-release nutrient carriers, which can improve nutrient utilisation efficiency.

TABLE-9
FIRST-ORDER RELEASE RATE CONSTANTS (k, day^{-1}) AND r^2 FOR CONVENTIONAL *vs*. FORTIFIED HYDROGELS (FITTED TO DAY 0, 7, 60; DATA; $M_t/M_\infty = 1 - e^{-kt}$)

Nutrient	k_{conv} (day^{-1})	r^2_{conv}	k_{hydro} (day^{-1})	r^2_{hydro}
B	0.35	0.995	0.24	0.985
Fe	0.33	0.999	0.23	0.987
Cu	0.27	0.995	0.20	0.968
Mn	0.36	1.000	0.24	0.993
Zn	0.43	1.000	0.27	0.995
MNM	0.30	0.990	0.22	0.980

Soil incubation further supported the controlled-release behaviour under a soil-based extraction system. At 60 days, cumulative release from hydrogel treatments remained lower than corresponding conventional sources for Zn, Fe, Mn, Cu and MNM treatments, indicating slower nutrient availability from the GGB matrix. However, since the soil release dataset was interpreted as a time-series release profile, the results are discussed descriptively along with kinetic fitting rather than as replicate-level two-way ANOVA.

Pot trials on *V. radiata*: The soil used for the pot experiment was alkaline in nature (pH 7.58) with low electrical conductivity (0.21 dS m^{-1}) indicating non-saline conditions. Organic carbon content was moderate (0.46%), while available P (19.80 kg ha^{-1}) and K (182.56 kg ha^{-1}) were in the low to medium range. Analysis of available micronutrients showed that Zn (0.59 mg kg^{-1}) was slightly deficient and B (0.35 mg kg^{-1}) was severely deficient, whereas Fe (3.48 mg kg^{-1}), Mn (4.02 mg kg^{-1}) and Cu (0.81 mg kg^{-1}) were present in sufficient quantities. The existing nutrient status of the soil, particularly the deficiencies of B and Zn, provided an appropriate basis for assessing the effectiveness of micronutrient-fortified hydrogel treatments. One-way ANOVA revealed significant differences among treatments for germination and plant growth parameters.

Germination: The germination percentages of *V. radiata* displayed significant variation among treatments at both observation stages. In control, the minimum germination rates of 45.0% and 66.7% indicate insufficient nutrient availability and moisture retention during the initial development phase. Among the treatments with nutrient application, treatment with the use of only RDF alone (T_1) achieved germination percentages of 58.3% at the initial stage and 75.0% at the final stage. Treatments with RDF and conventional micronutrient fertilizers (T_2, T_4, T_6, T_8, T_{10} and T_{12}) demonstrated enhanced germination at both stages, reaching 58-70% in the initial stage and 78-85% in the final stage. Conversely, treatments using RDF with fortified-GGB-hydrogels (T_3, T_5, T_7, T_9, T_{11} and T_{13}) exhibited improved germination, reaching 72-92% at the initial stage and 85-100% at the final stage. The maximum germination rate was recorded in treatment T_7 (MNM–GGB), reaching 91.7% on the seventh day and 100% on the 10th day, reflecting a 33% enhancement compared to the absolute control and a 25% improvement over RDF alone (Fig. 9).

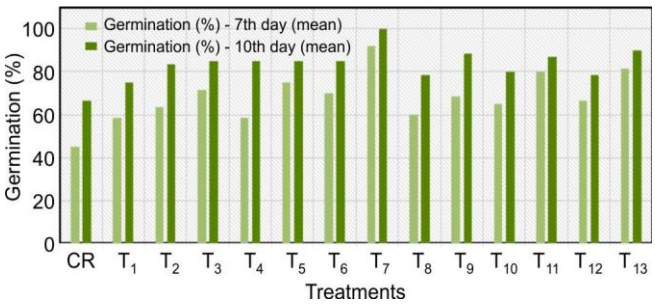

Fig. 9. Germination % of *V. radiata* on first (7th day) and final count (10th day) (mean of three replications)

Hence, it can be stated that the fortified hydrogel-based treatments excelled in both germination stages. The improved germination and early growth may be associated with the water-absorbing nature of the hydrogel matrix, as indicated by swelling behaviour, together with gradual nutrient release near the root zone. Soil water-retention capacity, mechanical strength and rheological properties were not directly quantified in the present work; therefore, these aspects should be evaluated in future studies.

Morphological plant growth parameters: The results of the study to understand the impact of conventional micronutrient fertilizers *vs.* fortified hydrogels on plant growth parameters of *V. radiata* are summarised in Table-10. One-way ANOVA showed a significant treatment effect on final germination percentage ($F = 12.56$, $p < 0.001$), root length ($F = 43.07$, $p < 0.001$), shoot length ($F = 50.64$, $p < 0.001$), plant

TABLE-10
EFFECT OF FERTILIZERS AND FORTIFIED HYDROGELS ON MORPHOLOGICAL PARAMETERS OF *V. radiata* AFTER 60 DAYS

Parameter	Final germination count	Root length (cm)	Shoot length (cm)	Plant height (cm)	Vigor index
A.C.	66.67 ± 2.89	2.23 ± 0.25	8.27 ± 0.25	10.50 ± 0.50	700.0 ± 44.4
T_1	75.00 ± 5.00	3.00 ± 0.20	9.50 ± 0.30	12.50 ± 0.50	938.3 ± 88.9
T_2	83.33 ± 2.89	3.73 ± 0.25	11.00 ± 0.50	14.50 ± 0.50	1229.0 ± 100.3
T_3	85.00 ± 5.00	4.77 ± 0.25	13.00 ± 0.50	17.33 ± 0.76	1509.0 ± 82.4
T_4	85.00 ± 5.00	3.50 ± 0.20	10.37 ± 0.40	13.50 ± 0.50	1176.7 ± 18.8
T_5	85.00 ± 5.00	5.03 ± 0.25	13.73 ± 0.50	18.77 ± 0.75	1596.3 ± 138.0
T_6	85.00 ± 5.00	3.60 ± 0.20	10.60 ± 0.40	14.00 ± 0.50	1208.0 ± 104.4
T_7	100.00 ± 0.00	4.87 ± 0.25	13.00 ± 0.40	18.00 ± 0.50	1786.7 ± 65.1
T_8	78.33 ± 2.89	3.40 ± 0.20	10.10 ± 0.30	13.50 ± 0.50	1058.3 ± 74.9
T_9	88.33 ± 2.89	4.60 ± 0.20	12.50 ± 0.40	17.00 ± 0.50	1510.5 ± 73.2
T_{10}	80.00 ± 5.00	3.30 ± 0.20	10.00 ± 0.30	13.30 ± 0.50	1064.8 ± 94.6
T_{11}	86.67 ± 2.89	4.50 ± 0.20	12.30 ± 0.40	16.80 ± 0.60	1457.0 ± 97.8
T_{12}	78.33 ± 2.89	3.20 ± 0.20	9.87 ± 0.35	13.03 ± 0.55	1022.7 ± 24.1
T_{13}	90.00 ± 0.00	4.40 ± 0.20	12.03 ± 0.35	16.50 ± 0.50	1479.0 ± 49.6
Parameter	Leaf length (cm)	Leaf width (cm)	Leaf area (cm^2)	Fresh biomass (g)	Dry biomass (g)
A.C.	2.90 ± 0.10	1.60 ± 0.17	3.48 ± 0.40	0.1027 ± 0.0422	0.0246 ± 0.0047
T_1	4.53 ± 0.31	2.00 ± 0.10	6.82 ± 0.79	0.1254 ± 0.0113	0.0326 ± 0.0061
T_2	4.10 ± 0.26	2.03 ± 0.15	6.27 ± 0.88	0.1377 ± 0.0021	0.0293 ± 0.0054
T_3	5.00 ± 0.20	2.30 ± 0.10	8.64 ± 0.72	0.1116 ± 0.0114	0.0327 ± 0.0034
T_4	5.03 ± 0.25	2.23 ± 0.25	8.46 ± 1.38	0.1341 ± 0.0188	0.0395 ± 0.0026
T_5	6.23 ± 0.25	3.00 ± 0.10	13.99 ± 1.10	0.1937 ± 0.0319	0.0505 ± 0.0029
T_6	5.23 ± 0.15	2.40 ± 0.10	9.43 ± 0.62	0.1584 ± 0.0013	0.0398 ± 0.0016
T_7	6.13 ± 0.15	2.90 ± 0.10	13.34 ± 0.74	0.2019 ± 0.0164	0.0523 ± 0.0047
T_8	5.03 ± 0.15	2.30 ± 0.10	8.69 ± 0.64	0.1434 ± 0.0039	0.0379 ± 0.0017
T_9	5.73 ± 0.15	2.70 ± 0.10	11.61 ± 0.72	0.1859 ± 0.0081	0.0503 ± 0.0036
T_{10}	4.93 ± 0.15	2.20 ± 0.10	8.15 ± 0.62	0.1481 ± 0.0074	0.0410 ± 0.0021
T_{11}	5.63 ± 0.15	2.60 ± 0.10	10.99 ± 0.72	0.1774 ± 0.0142	0.0490 ± 0.0043
T_{12}	4.83 ± 0.15	2.10 ± 0.10	7.62 ± 0.60	0.1430 ± 0.0119	0.0378 ± 0.0025
T_{13}	5.60 ± 0.10	2.63 ± 0.06	11.06 ± 0.42	0.1697 ± 0.0106	0.0451 ± 0.0027

height ($F = 57.79$, $p < 0.001$), vigour index ($F = 40.10$, $p < 0.001$), leaf area ($F = 39.71$, $p < 0.001$), fresh biomass ($F = 8.95$, $p < 0.001$) and dry biomass ($F = 16.00$, $p < 0.001$).

The assessment of plant growth parameters in *V. radiata* indicated that the root length, shoot length and plant height in the control were 2.23 cm, 8.27 cm and 10.5 cm, respectively. In T_5 (Zn-GGB), these values increased to 5.03 cm, 13.73 cm and 18.77 cm, indicating improved plant growth under treatment. The vigor index is an integrated parameter of % germination and seedling length and is widely used to assess early physiological performance and field establishment potential [32]. In the present pot trial study, vigor index in absolute control is found to be 700, which increased to 938 in treatment T_1 of RDF. This indicates the positive impact of supplied N and P fertilisation by urea and DAP. Conventional micronutrient treatments further improved vigor index to 1023-1229, confirming the contribution of balanced nutrition. However, the highest values of the vigor index were recorded in fortified hydrogel treatments, ranging from 1457 to 1787, particularly MNM-GGB (1787) and Zn-GGB (1596). These results indicate that fortified-GGB-hydrogels were more effective for improving early seedling vigor, likely because they retained soil moisture and ensured a gradual release of the nutrients. Leaf characteristics also followed a similar pattern. In absolute control treatment, plants showed the smallest leaves, with mean leaf length, width and area of 2.9 cm, 1.6 cm and 3.48 cm^2, respectively, whereas RDF alone showed nearly doubled leaf area at 6.82 cm^2. Conventional micronutrient treatments displayed increased leaf area to 6.27-9.43 cm^2, with Zn-EDTA and the micronutrient mix showing comparatively better performance. The largest leaves were observed in the treatment of fortified hydrogels, where the leaf area ranged from 8.64 to 13.99 cm^2, with Zn-GGB and MNM-GGB producing the biggest leaves. Fresh and dry biomass after harvest also supported these results. The absolute control recorded the lowest fresh biomass of 0.1027 g and 0.0246 g of dry weight per plant, while treatment with RDF alone improved these values to 0.1254 g and 0.0326 g. The conventional micronutrient treatments produced plants with fresh biomass ranging from 0.1341 to 0.1584 g and dry biomass from 0.0293 to 0.0398 g. In contrast, fortified hydrogel treatments gave the highest biomass, with Zn-GGB and MNM-GGB showing the best performance. Fresh biomass ranged from 0.1697 to 0.2019 g and dry biomass ranged from 0.0451

to 0.0523 g, indicating significant improvements compared to both the control and conventional micronutrient fertilizer treatments, as well as RDF. These findings suggest that fortified GGB hydrogels, particularly MNM-GGB, enhanced early growth and establishment of *V. radiata* by improving soil moisture retention and ensuring sustained micronutrient availability in the root zone. These combined effects promoted root development, plant height, leaf growth and total vegetative performance.

Post-harvest soil study: Post-harvest soil analysis was conducted to test the residual status of nutrients after harvest to support the nutrient release behaviour observed in the soil-release study [33]. Mean values of post-harvest soil properties for all treatments are shown in Table-11. Soil pH (7.46-7.56) and EC (~0.21-0.23 dS m^{-1}) varied only slightly among the treatments and remained within a similar range throughout the study. These results show that the application of fortified hydrogels did not alter soil reaction or contribute to salt accumulation in the soil.

Compared with the initial soil, the absolute control showed reductions in available P, K, S and micronutrient concentrations, reflecting nutrient uptake by the crop without external nutrient supplementation. Treatments receiving RDF along with conventional micronutrient sources generally maintained nutrient levels, whereas hydrogel-based treatments, particularly the MNM-GGB treatment (T_7), retained higher residual concentrations of P, K and micronutrients after harvest. The higher residual levels of Zn, Mn and B in hydrogel-treated soils are consistent with the sustained nutrient-release behaviour observed in the release studies. These results highlight the ability of fortified GGB hydrogels to provide a continuous nutrient supply while maintaining nutrient availability in the soil after crop growth.

Statistical analysis revealed significant treatment effects on OC ($F = 21.43$, $p < 0.001$), pH ($F = 10.60$, $p < 0.001$), P ($F = 97.90$, $p < 0.001$), K ($F = 108.00$, $p < 0.001$), S ($F = 48.85$, $p < 0.001$), Zn ($F = 6.24$, $p < 0.001$), Fe ($F = 433.30$, $p < 0.001$), Mn ($F = 486.31$, $p < 0.001$), Cu ($F = 30.62$, $p <$

TABLE-11
POST-HARVEST SOIL PROPERTIES OF *V. radiata* POT TRIALS (MEAN OF THREE REPLICATIONS)

Code	Treatment description	pH	EC (dS m^{-1})	OC (%)	P (kg ha^{-1})	K (kg ha^{-1})
Initial soil	Before sowing	7.58	0.21	0.46	19.80	182.56
AC	Soil only	7.53 ± 0.01	0.21 ± 0.01	0.45 ± 0.01	18.27 ± 0.09	169.00 ± 1.65
T_1	RDF (urea + DAP)	7.55 ± 0.01	0.22 ± 0.01	0.44 ± 0.01	18.79 ± 0.15	174.33 ± 0.89
T_2	RDF + B (DOT)	7.53 ± 0.01	0.23 ± 0.01	0.45 ± 0.01	19.15 ± 0.11	177.31 ± 0.95
T_3	RDF + GGB hydrogel	7.51 ± 0.01	0.22 ± 0.01	0.44 ± 0.01	18.96 ± 0.11	175.48 ± 0.93
T_4	RDF + Zn-EDTA	7.50 ± 0.01	0.22 ± 0.01	0.44 ± 0.01	19.16 ± 0.12	177.31 ± 1.13
T_5	RDF + Zn-GGB hydrogel	7.52 ± 0.01	0.23 ± 0.01	0.45 ± 0.01	18.85 ± 0.13	175.52 ± 0.87
T_6	RDF + Micronutrient mix	7.53 ± 0.02	0.23 ± 0.01	0.44 ± 0.01	17.75 ± 0.17	161.43 ± 2.07
T_7	RDF + MNM-GGB hydrogel	7.50 ± 0.02	0.22 ± 0.01	0.45 ± 0.01	18.45 ± 0.20	167.45 ± 0.79
T_8	RDF + $FeSO_4$	7.50 ± 0.02	0.22 ± 0.01	0.45 ± 0.01	18.93 ± 0.14	170.46 ± 0.97
T_9	RDF + Fe-GGB hydrogel	7.53 ± 0.02	0.23 ± 0.01	0.46 ± 0.01	19.28 ± 0.10	173.36 ± 0.90
T_{10}	RDF + $CuSO_4$	7.49 ± 0.01	0.23 ± 0.01	0.47 ± 0.01	19.56 ± 0.07	178.62 ± 1.12
T_{11}	RDF + Cu-GGB hydrogel	7.48 ± 0.01	0.22 ± 0.01	0.47 ± 0.01	19.75 ± 0.10	181.47 ± 0.79
T_{12}	RDF + $MnSO_4$	7.50 ± 0.01	0.23 ± 0.01	0.48 ± 0.01	20.06 ± 0.11	183.56 ± 0.78
T_{13}	RDF + Mn-GGB hydrogel	7.47 ± 0.01	0.23 ± 0.01	0.50 ± 0.01	20.48 ± 0.10	186.47 ± 0.83
Code	Treatment description	Zn (mg kg^{-1})	Fe (mg kg^{-1})	Mn (mg kg^{-1})	Cu (mg kg^{-1})	B (mg kg^{-1})
Initial soil	Before sowing	0.59	3.48	4.02	0.81	0.35
AC	Soil only	0.58 ± 0.01	3.41 ± 0.01	3.88 ± 0.02	0.80 ± 0.01	0.34 ± 0.01
T_1	RDF (urea + DAP)	0.57 ± 0.02	3.39 ± 0.02	3.85 ± 0.01	0.79 ± 0.01	0.34 ± 0.01
T_2	RDF + B (DOT)	0.59 ± 0.02	3.46 ± 0.01	3.89 ± 0.01	0.80 ± 0.01	0.35 ± 0.01
T_3	RDF + GGB hydrogel	0.59 ± 0.01	3.56 ± 0.01	3.92 ± 0.01	0.80 ± 0.01	0.34 ± 0.00
T_4	RDF + Zn-EDTA	0.58 ± 0.01	3.49 ± 0.01	4.05 ± 0.01	0.80 ± 0.01	0.34 ± 0.01
T_5	RDF + Zn-GGB hydrogel	0.58 ± 0.01	3.41 ± 0.01	3.88 ± 0.01	0.85 ± 0.01	0.34 ± 0.00
T_6	RDF + Micronutrient mix	0.55 ± 0.02	3.33 ± 0.02	3.49 ± 0.03	0.77 ± 0.01	0.32 ± 0.01
T_7	RDF + MNM-GGB hydrogel	0.57 ± 0.02	3.43 ± 0.02	3.67 ± 0.03	0.79 ± 0.01	0.34 ± 0.00
T_8	RDF + $FeSO_4$	0.57 ± 0.01	3.62 ± 0.01	3.86 ± 0.01	0.78 ± 0.01	0.33 ± 0.01
T_9	RDF + Fe-GGB hydrogel	0.57 ± 0.01	3.51 ± 0.01	4.09 ± 0.01	0.79 ± 0.01	0.34 ± 0.01
T_{10}	RDF + $CuSO_4$	0.60 ± 0.02	3.63 ± 0.01	3.98 ± 0.01	0.82 ± 0.01	0.35 ± 0.01
T_{11}	RDF + Cu-GGB hydrogel	0.61 ± 0.01	3.71 ± 0.01	4.01 ± 0.02	0.81 ± 0.01	0.35 ± 0.00
T_{12}	RDF + $MnSO_4$	0.60 ± 0.01	3.62 ± 0.01	4.15 ± 0.01	0.81 ± 0.01	0.35 ± 0.01
T_{13}	RDF + Mn-GGB hydrogel	0.62 ± 0.02	3.82 ± 0.01	4.20 ± 0.01	0.83 ± 0.01	0.37 ± 0.01

0.001) and B (F = 17.11, $p < 0.001$). In contrast, electrical conductivity was not significantly affected by treat-ment (F = 1.52, p = 0.173), indicating that hydrogel appli-cation did not contribute to soil salinity. Although organic carbon varied significantly among treatments, the magnitude of change was relatively small. Thus, the post-harvest soil analysis revealed that fortified GGB hydrogels maintained nutrient availability more effectively than conventional micronutrient sources, highlighting their potential as slow-release nutrient carriers for sustainable crop production.

Although organic carbon varied significantly among treatments, the magnitude of change was relatively small, reflecting minimal alteration of the chemical characteristics of soil following hydrogel application. While the study included absolute control, RDF control, blank GGB hydrogel control and nutrient-matched conventional micronutrient treatments, future research incorporating guar gum-only controls, non-EDTA micronutrient sources, commercial fertilizer products and field-scale evaluations would provide a more comprehensive assessment of the agronomic potential of fortified GGB.

Conclusion

In this work, the elemental analysis confirmed efficient incorporation of B, Fe, Zn, Cu, Mn and multi-micronutrient formulations into the guar gum-borax (GGB) hydrogel through the post-gelation loading approach. The structural, thermal, crystallinity and morphological analyses verified successful micronutrient integration while preserving the integrity of the guar gum-borax network. The fortified hydrogels exhibited sustained nutrient release in aqueous media and prolonged micronutrient availability in soil compared with conventional nutrient sources. Their water absorption capacity further contributed to diffusion-controlled nutrient release. In *V. radiata* pot experiments, fortified hydrogels enhanced or maintained germination and vegetative growth relative to RDF and conventional micronutrient treatments, while post-harvest soil analysis showed stable pH and EC with improved micronutrient availability. These findings highlight the potential of fortified GGB hydrogels as biodegradable carriers for controlled micronutrient delivery; however, field-scale evaluation and long-term studies on rheological properties and soil biological responses are needed to establish their wider agronomic applicability.

ACKNOWLEDGEMENTS

The authors thank the Analytical & Advanced Instrumentation Laboratory of GSFC University, Vadodara and Gujarat State Fertilizers & Chemicals Limited, Vadodara, for providing support and research facilities.

CONFLICT OF INTEREST

The authors declare that there is no conflict of interests regarding the publication of this article.

DECLARATION OF AI-ASSISTED TECHNOLOGIES

During the preparation of this manuscript, the authors used an AI-assisted tool(s) to improve the language. The authors reviewed and edited the content and take full responsibility for the published work.

REFERENCES

1. N. Ahmed, B. Zhang, Z. Chachar, J. Li, G. Xiao, Q. Wang, F. Hayat, L. Deng, M.-N. Narejo, B. Bozdar and P. Tu, *Sci. Hortic.*, **323**, 112512 (2024); https://doi.org/10.1016/j.scienta.2023.112512
2. L. Galić, V. Vukadinović, I. Nikolin and Z. Lončarić, *Crops*, **5**, 40 (2025); https://doi.org/10.3390/crops5040040
3. L.E. Hernandez, J.M. Ruiz, F. Espinosa, A. Alvarez-Fernandez and M. Carvajal, *Physiol. Plant.*, **176**, e70018 (2024); https://doi.org/10.1111/ppl.70018
4. R. Hänsch and R.R. Mendel, *Curr. Opin. Plant Biol.*, **12**, 259 (2009); https://doi.org/10.1016/j.pbi.2009.05.006
5. L.V.P. Minello, S.G. Kuntzler, E. Berghahn, L.T. Dorneles, F.K. Ricachenevsky and R.A. Sperotto, *J. Nanobiotechnology*, **23**, 669 (2025); https://doi.org/10.1186/s12951-025-03746-8
6. A. Nongbet, A.K. Mishra, Y.K. Mohanta, S. Mahanta, M.K. Ray, M. Khan, K.H. Baek and I. Chakrabartty, *Plants*, **11**, 2587 (2022); https://doi.org/10.3390/plants11192587
7. A.K. Bhardwaj, S. Chejara, K. Malik, R. Kumar, A. Kumar and R.K. Yadav, *Front. Plant Sci.*, **13**, 1055278 (2022); https://doi.org/10.3389/fpls.2022.1055278
8. N.H. Thang, T.B. Chien and D.X. Cuong, *Gels*, **9**, 523 (2023); https://doi.org/10.3390/gels9070523
9. R. Ene (Vatcu), A.-T. Iacob, I. Fulga, M.L. Di Gioia, I. Dragostin, A. Fulga, S.K. Samal and O.-M. Dragostin, *Polymers*, **18**, 709 (2026); https://doi.org/10.3390/polym18060709
10. D. Nanda, D. Behera, S.S. Pattnaik and A.K. Behera, *Discov. Polym.*, **2**, 6 (2025); https://doi.org/10.1007/s44347-025-00017-5
11. Y. Flores García, M.F. Martín Del Campo Solís, J.H. Gómez-Angulo, A.H. Martínez Preciado, J.M. Silva-Jara, J.D. Padilla de la Rosa and Z.Y. Escalante-Garcia, *Foods*, **14**, 1587 (2025); https://doi.org/10.3390/foods14091587
12. T. Le and T. Huynh, *Eur. Polym. J.*, **184**, 111852 (2023); https://doi.org/10.1016/j.eurpolymj.2023.111852
13. Y. Bachra, A. Grouli, F. Damiri, X.X. Zhu, M. Talbi and M. Berrada, *ACS Omega*, **7**, 39002 (2022); https://doi.org/10.1021/acsomega.2c04744
14. G. Patroklou, E. Triantafyllopoulou, P.-E. Goula, M. Chountoulesi, V. Karali, G. Valsami, S. Pispas and N. Pippa, *Polymers*, **17**, 1451 (2025); https://doi.org/10.3390/polym17111451
15. X. Zhang, X. Kan, Y. Xie, Y. Wang, Z. Li, X. Lun, Y. Zhao, S. Zhang, N. Wu and W. Xu, *Ind. Crops Prod.*, **235**, 121804 (2025); https://doi.org/10.1016/j.indcrop.2025.121804
16. X. Chen, N. Ji, F. Li, Y. Qin, Y. Wang, L. Xiong and Q. Sun, *Foods*, **11**, 1315 (2022); https://doi.org/10.3390/foods11091315
17. N. Thombare, S. Mishra, R. Shinde, M.Z. Siddiqui and U. Jha, *Biopolymers*, **112**, e23418 (2021); https://doi.org/10.1002/bip.23418
18. T.O. Machado, J. Grabow, C. Sayer, P.H.H. de Araújo, M.L. Ehrenhard and F.R. Wurm, *Adv. Colloid Interface Sci.*, **303**, 102645 (2022); https://doi.org/10.1016/j.cis.2022.102645
19. C. Buitrago-Arias, P. Gañán-Rojo, M. Torres-Taborda, L. Perdomo-Villar, C. Álvarez-López, N. Jaramillo-Quiceno and G.A. Hincapié-Llanos, *Gels*, **11**, 731 (2025); https://doi.org/10.3390/gels11090731
20. A. Ravindran, A.C. Manivannan, R. Kandaiah, M. Kulanthaisamy, S.C. Indirathankam, G. Nachimuthu, L. Panneerselvan and T. Palanisami, *Ind. Crops Prod.*, **233**, 121349 (2025); https://doi.org/10.1016/j.indcrop.2025.121349

21. M.S. Haydar, D. Ghosh and S. Roy, *Plant Nano Biol.*, **7**, 100058 (2024); https://doi.org/10.1016/j.plana.2024.100058
22. M.M. Bhuyan and J.H. Jeong, *Gels*, **11**, 896 (2025); https://doi.org/10.3390/gels11110896
23. A. Berradi, F. Aziz, M.E. Achaby, N. Ouazzani and L. Mandi, *Polymers*, **15**, 2908 (2023); https://doi.org/10.3390/polym15132908
24. N. Thombare, U. Jha, S. Mishra and M.Z. Siddiqui, *Carbohydr. Polym.*, **168**, 274 (2017); https://doi.org/10.1016/j.carbpol.2017.03.086
25. N. Manousi, E. Isaakidou and G.A. Zachariadis, *Appl. Sci.*, **12**, 534 (2022); https://doi.org/10.3390/app12020534
26. M. Senila, *Molecules*, **29**, 3169 (2024); https://doi.org/10.3390/molecules29133169
27. N. Thombare, U. Jha, S. Mishra and M.Z. Siddiqui, *Int. J. Biol. Macromol.*, **88**, 361 (2016); https://doi.org/10.1016/j.ijbiomac.2016.04.001
28. G.M. Estrada-Villegas, G. Morselli, M.J.A. Oliveira, G. González-Pérez and A.B. Lugão, *Polym. Bull.*, **77**, 1 (2020); https://doi.org/10.1007/s00289-019-02966-x
29. M. Hussain, T. Zahoor, S. Akhtar, A. Ismail and A. Hameed, *J. Food Sci. Technol.*, **55**, 1047 (2018); https://doi.org/10.1007/s13197-017-3018-5
30. A. Kaur, D. Singh and D. Sud, *J. Polym. Res.*, **27**, 297 (2020); https://doi.org/10.1007/s10965-020-02271-6
31. S. Van Vlierberghe, P. Dubruel and E. Schacht, *Biomacromolecules*, **12**, 1387 (2011); https://doi.org/10.1021/bm200083n
32. K. Ali, Z. Asad, G.H.D. Agbna, A. Saud, A. Khan and S.J. Zaidi, *Agronomy*, **14**, 2815 (2024); https://doi.org/10.3390/agronomy14122815
33. S. Dwivedi, A. Srivastava, S.P. Gangwar, P. Dey, P. Dey, M.K. Bhatt, S. Sarkar, P. Bhattacharya, D. Mandal, M. Alotaibi and M.F. Seleiman, *BMC Plant Biol.*, **24**, 1203 (2024); https://doi.org/10.1186/s12870-024-05890-z